

State-space Modeling of Multi-mode-controlled Induction Motor Drive

Zhe Zhang, Muhammed Ali Gultekin, Ali M. Bazzi, *Senior Member, IEEE*
 Department of Electrical and Computer Engineering, University of Connecticut, USA
 zhe.4.zhang@uconn.edu

Abstract— The theory of switched systems which focuses on stability and control synthesis of systems with multiple modes or different dynamics, has gained significant attention from control theorists, computer scientists, and practicing engineers. Switching between motor controllers due to sensor faults, faster response, or targeted dynamics, open a new dimension of shaping a motor drive’s performance. There are three main types of control strategies for induction motor drives: constant volts per hertz (V/f) control, field-oriented control (FOC), and direct torque control (DTC). Multi-mode-controlled induction motor drive can be modelled as a switched system where each control mode results in different motor dynamics. In this paper, a comprehensive state-space model of an induction motor drive under different control mode is developed. Detailed analysis as well as simulation results are included to demonstrate the validity of the state-space representation for induction motor under different mode.

Keywords—induction motor drive, switched system, switched control, state-space representation, multi-mode control.

I. INTRODUCTION

Induction motors (IMs) are widely used in electrical drives because of their ruggedness and relatively low cost. Scalar control, namely constant volts per hertz (V/f) control [1], offers the simplest solution in applications such as pumps, compressors, heating, ventilation, and air conditioning, where the transient performance of the motor is not of great concern. It also relies on no or minimal number of sensors. On the other hand, closed-loop vector control techniques such as indirect field-oriented control (IFOC) and direct torque control (DTC) have also been well-established for high-performance adjustable speed drives (ASDs). All three control modes can be integrated in one electrical drive due to the enhanced computing power of digital signal processors (DSPs), which makes the whole drive more robust and can withstand sensor failures, giving engineers and operators flexibility on shaping a drive’s response.

A switched system has hybrid dynamic features. It consists of a finite number of subsystems described by discrete (or continuous) time dynamics and a switching rule governing the switching among them. A typical architecture of a multi-controller switched system is shown in Fig. 1. A high-level decision maker (supervisor) determines which controller is to be connected in closed loop with the plant at each instant of time [5]. Fig. 2 illustrates the system architecture of an induction motor (IM) drive with three admissible modes. Since the IM drive exhibits different dynamics depending on the selected mode, it can be

modeled as a switched system. Three subsystems are embedded within the switched system: V/f-controlled, IFOC-controlled, and DTC-controlled IM drive.

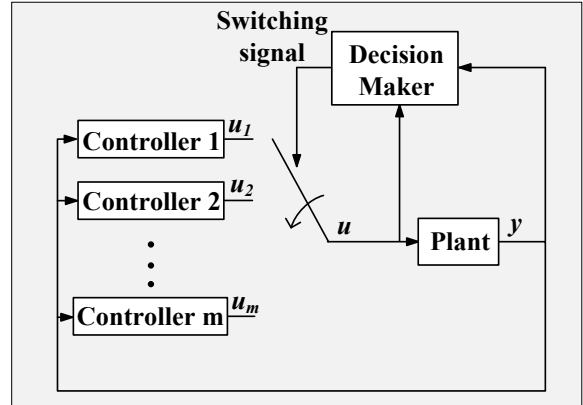


Fig. 1. A Multi-controller switched system.

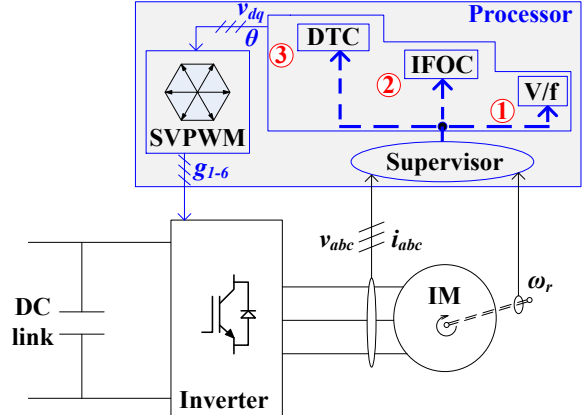


Fig. 2. System architecture of a multi-mode induction motor drive.

V/f control is essentially an open-loop control scheme and will be kept as the fundamental mode. IFOC or DTC will serve as advanced modes that the electrical drive can be switched to when superior drive performance is desired, depending on sensor availability and health. The block diagram for all three control modes is shown in Fig. 3. (a), (b), and (c), respectively [2], [3]. There is a supervisory controller within the processor that continuously monitors the system’s states and determines which mode to select [4]. As far as the stability with arbitrary switching is concerned, it is necessary to require that all the subsystems be asymptotically stable. However, even when all the subsystems of a switched system are stable, such a system might fail to preserve stability under arbitrary switching but might be stabilized under restricted switching signals [6].

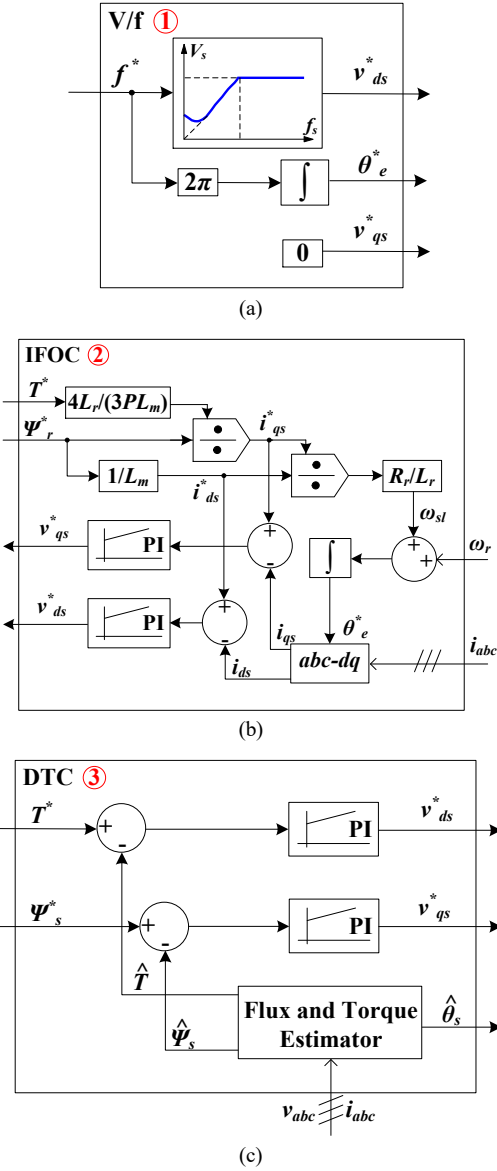


Fig. 3. Block diagram of different control strategies: (a) V/f control; (b) IFOC; (c) DTC.

Among the tools that have been developed for stability analysis of switched systems, the notion of dwell-time or average dwell-time (ADT) has played a significant role in characterization of stability conditions [7]. Unfortunately, none of the existing literatures have investigated IM drive stability under different modes in the context of switching control. In [8], the lower bounds on ADT which guarantee input-to-state stability (ISS) is derived within the context of stability of switched systems under slow switching. The framework proposed in [8] has provided a tool to analyze the optimal ADT that ensures stable operation of multi-mode-controlled IM drive. Before we can apply the framework to the IM drive, each subsystem's dynamics must be identified first.

The rest of the paper is organized as follows: Section II presents the workflow in developing the state-space representation of motor dynamics under each controller; Section III includes the simulation results to show the validity of the proposed state-space representation of motor dynamics under each controller; Section IV concludes the paper.

II. STATE-SPACE MODELING OF INDUCTION MOTOR DRIVE UNDER DIFFERENT CONTROL MODES

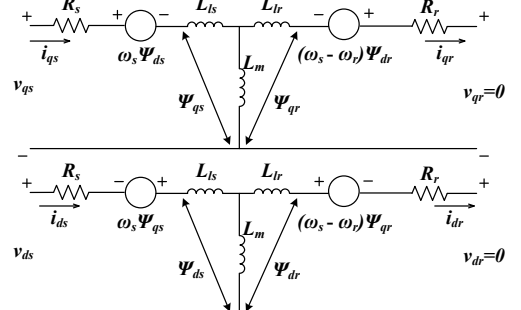


Fig. 4. Dynamic equivalent circuit of an IM in d - q frame [9].

In this section, we will be closely looking into the problem that how the IM drive under different control modes can be modeled as linear switched systems. Fig. 4 shows the dynamic equivalent circuit of a squirrel cage induction motor in the synchronous reference frame. Such equivalent circuit can be described by a set of fifth order non-linear differential equations:

$$\begin{aligned}
 \dot{\Psi}_{qs} &= -\frac{R_s}{\chi_3} \Psi_{qs} - \omega_s \Psi_{ds} - \frac{R_s}{\chi_1} \Psi_{qr} + v_{qs} \\
 \dot{\Psi}_{ds} &= \omega_s \Psi_{qs} - \frac{R_s}{\chi_3} \Psi_{ds} - \frac{R_s}{\chi_1} \Psi_{dr} + v_{ds} \\
 \dot{\Psi}_{qr} &= -\frac{R_r}{\chi_1} \Psi_{qs} - \frac{R_r}{\chi_2} \Psi_{qr} - (\omega_s - \omega_r) \Psi_{dr} \\
 \dot{\Psi}_{dr} &= -\frac{R_r}{\chi_1} \Psi_{ds} + (\omega_s - \omega_r) \Psi_{qr} - \frac{R_r}{\chi_2} \Psi_{dr} \\
 J \dot{\omega}_r &= \frac{3P}{2\chi_1} (\Psi_{ds} \Psi_{qr} - \Psi_{qs} \Psi_{dr}) - T_L \\
 \chi_1 &= L_m - L_s L_r / L_m \\
 \chi_2 &= L_r - L_m^2 / L_s \\
 \chi_3 &= L_s - L_m^2 / L_r
 \end{aligned} \tag{8}$$

where subscript d and q denote direct and quadrature axis, respectively; subscript s and r denote stator and rotor, respectively; R represents the resistance; L represents the inductance; Ψ represents the flux linkage; ω represents electrical frequency; L_m is the magnetizing inductance; P is pole pair of an IM; J and T_L are moment of inertia and applied mechanical torque on the shaft, respectively.

Based on the equivalent circuit, the state-space representations of V/f control, IFOC, and DTC are developed in the following subsections. The inverter's non-linearities are ignored for simplicity. Realization of each control mode is the same as the block diagram shown in Fig. 3. Small-signal perturbation can be applied at a steady-state operating point to derive a linearized model for the IM drive under different control modes.

A. Motor Dynamics Under V/f control, IFOC, and DTC

For V/f control, according to Fig. 3 (a), the q -axis stator voltage v_{qs} is kept at zero, while the d -axis stator voltage v_{ds} is set proportional to ω_s . The motor dynamics under V/f control can be rewritten as:

$$\begin{aligned}
\dot{\psi}_{qs} &= -(R_s / \chi_3)\psi_{qs} - \omega_s \psi_{ds} - (R_s / \chi_1)\psi_{qr} \\
\dot{\psi}_{ds} &= \omega_s \psi_{qs} - (R_s / \chi_3)\psi_{ds} - (R_s / \chi_1)\psi_{dr} + k\omega_s \\
\dot{\psi}_{qr} &= -(R_r / \chi_1)\psi_{qs} - (R_r / \chi_2)\psi_{qr} - (\omega_s - \omega_r)\psi_{dr} \\
\dot{\psi}_{dr} &= -(R_r / \chi_1)\psi_{ds} + (\omega_s - \omega_r)\psi_{qr} - (R_r / \chi_2)\psi_{dr} \\
J\dot{\omega}_r &= (3P/2\chi_1)(\psi_{ds}\psi_{qr} - \psi_{qs}\psi_{dr}) - T_L
\end{aligned} \tag{9}$$

where $k = V_{rated}/\omega_{rated}$ defines the flux level.

Under IFOC, according to Fig. 3 (b), d -axis stator current i_{ds} is supposed to regulate the rotor flux, while q -axis stator current i_{qs} is supposed to control the electromagnetic torque. Therefore, decoupled control over rotor flux and electromagnetic torque can be achieved and the motor dynamics can be simplified as:

$$\begin{aligned}
\dot{\psi}_{dr} &= -(R_r / L_r)\psi_{dr} + (R_r L_m / L_r)i_{ds} \\
T_e &= (3P/2\chi_1)(L_m^2 / L_r - L_s)\psi_{dr}i_{qs}
\end{aligned} \tag{10}$$

In DTC, according to Fig. 3 (c), the stator is to be controlled instead by the d -axis stator voltage v_{ds} and the electromagnetic torque is to be regulated by the q -axis stator voltage v_{qs} accordingly. The motor dynamics reduce to

$$\begin{aligned}
\dot{\psi}_{ds} &= -(R_s / \chi_3)\psi_{ds} - (R_s / \chi_1)\psi_{dr} + v_{ds} \\
\dot{\psi}_{dr} &= -(R_r / \chi_1)\psi_{ds} - (R_r / \chi_2)\psi_{dr} \\
T_e &= (3P/2R_s)\psi_{ds}(v_{qs} - \omega_s \psi_{ds})
\end{aligned} \tag{11}$$

B. State-space Representation Derivation of IM Drive Under V/f Control/IFOC/DTC

To derive the state-space representation of the IM drive as a whole requires linearizing the motor dynamics at certain steady-state operating point and incorporating each controller's dynamics to make it a closed-loop system where applicable. Both IFOC and DTC adopt dual proportional-integral (PI) controllers to compensate for stator voltages. The transfer function of a general PI controller is:

$$\begin{aligned}
G(s) &= v / e \\
&= (v / u)(u / e) \\
&= (k_p s + k_i)(1 / s)
\end{aligned} \tag{12}$$

Rewrite eq. (12) as:

$$\begin{aligned}
\dot{u} &= e \\
v &= k_p \dot{u} + k_i u \\
&= k_p e + k_i u
\end{aligned} \tag{13}$$

where s is the Laplace operator; e and v represent the input and output of a PI controller, respectively; k_p and k_i represent the proportional gain and integral gain, respectively; u is an intermediate state variable associated with the input.

According to (10), the motor dynamics under IFOC are associated with stator currents. Since the motor is usually fed by a voltage source inverter (VSI) [10], [11], the relationships between stator voltages and stator currents under IFOC are approximated as:

$$\begin{aligned}
\frac{i_{qs}}{v_{qs}} &= \frac{1}{\chi_3 s + R_s} \\
\frac{i_{ds}}{v_{ds}} &= \frac{s + 1/T_r}{\chi_3 s^2 + [R_s + \chi_3/T_r + L_m/(T_m T_r)]s + R_s/T_r}
\end{aligned} \tag{14}$$

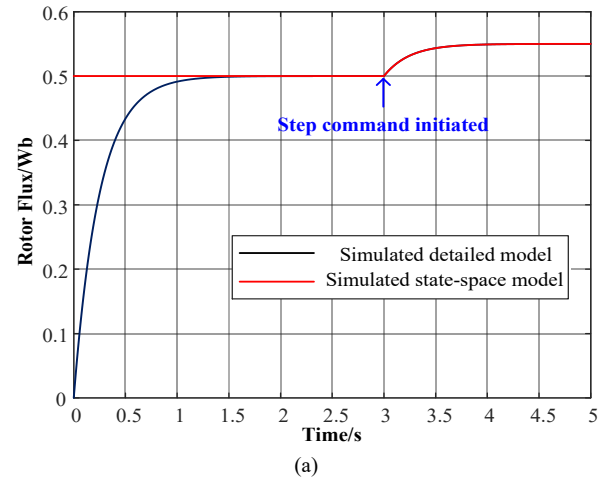
where $T_r = L_r/R_r$, and $T_m = L_r/L_m$.

Combining (9)-(14), the state-space representation (state matrix, input matrix, state variables and inputs) of IM drive under each control mode is summarized and shown in Table I. Note that subscript 0 denotes the steady-state operation point where small-signal perturbation is applied, and superscript * denotes the input command. The proportional and integral gains to regulate d - and q -axis currents in IFOC are denoted as $k_{p,d}$ and $k_{i,d}$, and $k_{i,q}$ and $k_{p,q}$, respectively. Similarly, the proportional and integral gains for regulations of flux and torque in DTC are denoted as $k_{p,\psi}$ and $k_{i,\psi}$, and $k_{i,T}$ and $k_{p,T}$, respectively.

III. MODEL VERIFICATION

A detailed model of the IM as well as all three controllers are simulated in MATLAB/Simulink. The IM parameters are given in Table II. In addition, the derived state-space representations for each control mode are simulated in MATLAB/Simulink to compare their response with the detailed ones'. Fig. 5 and Fig. 6 illustrate the simulated results for IM drive under IFOC and DTC, respectively. In IFOC, the rotor flux command is set to 0.5 Wb and torque command is set to 1.5 N.m. When the drive reaches its steady state, a 10% increase in both commanded rotor flux and torque is applied. As can be seen, the derived state-space model shows similar IM drive dynamics under IFOC to those from the detailed model.

The same step response is tested with detailed and derived state-space model for DTC. Overall, the derived state-space model reflects the dynamics of the IM drive under each control mode as expected.



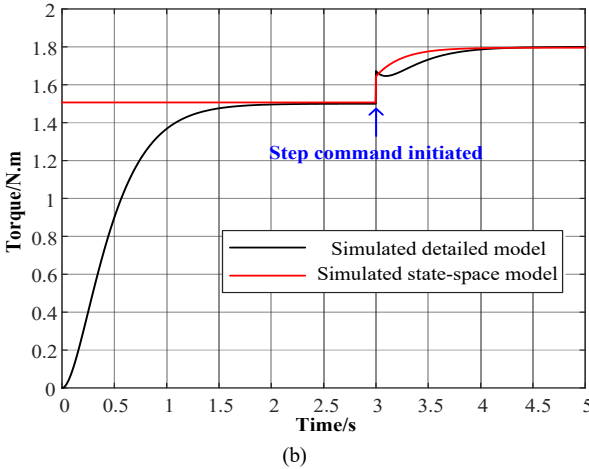


Fig. 5. Simulated step response for both detailed model and state-space model: (a) Rotor flux response under IFOC; (b) Torque response under IFOC.

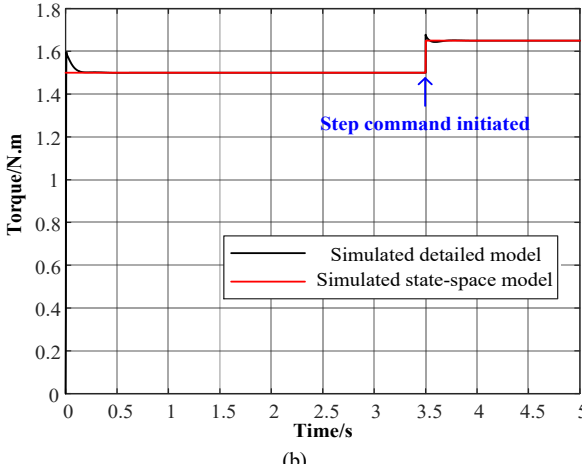
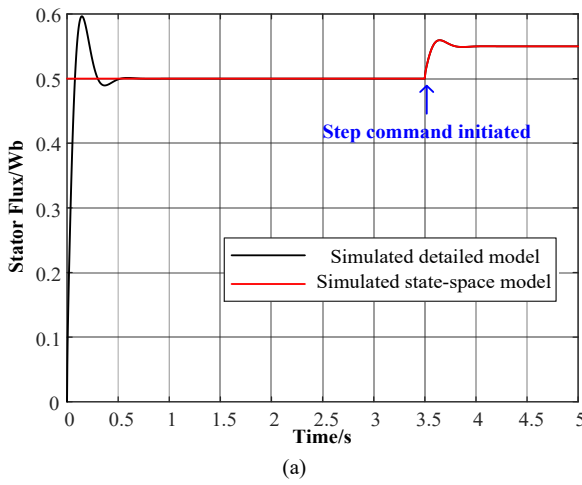


Fig. 6. Simulated step response for both detailed model and state-space model: (a) Stator flux response under DTC; (b) Torque response under DTC.

IV. CONCLUSIONS

In this paper, the IM drive under different control modes is modeled for use in switched system analysis. State-space model of the IM drive under three different control modes is developed and validated from simulations. The proposed model provides the recipes for analysis of multi-mode-controlled IM drive to further analyze ADT in stabilizing

switched systems. Further research on this topic will be reported in the future.

V. ACKNOWLEDGEMENT

This work is supported by the National Science Foundation under Award 1752297.

REFERENCES

- [1] Z. Zhang, Y. Liu and A. M. Bazzi, "An improved high-performance open-loop V/f control method for induction machines," *2017 IEEE Applied Power Electronics Conference and Exposition (APEC)*, Tampa, FL, 2017, pp. 615-619.
- [2] Z. Zhang and A. M. Bazzi, "Robust Sensorless Scalar Control of Induction Motor Drives with Torque Capability Enhancement at Low Speeds," *2019 IEEE International Electric Machines & Drives Conference (IEMDC)*, San Diego, CA, USA, 2019, pp. 1706-1710.
- [3] Z. Zhang, Z.G. Liu, L.T. Zhao, L.J. Diao, "Research on AC drive test system based on vector control," in *Proceedings of the 2013 International conference on Electrical and Information Technologies for Rail Transportation (EITRT2013)*, Vol. 288, 2014, pp. 537-546.
- [4] M. Stettenbenz, Y. Liu and A. Bazzi, "Smooth switching controllers for reliable induction motor drive operation after sensor failures," *2015 IEEE Applied Power Electronics Conference and Exposition (APEC)*, Charlotte, NC, 2015, PP. 2407-2411.
- [5] D. Liberzon and A. S. Morse, "Basic problems in stability and design of switched systems," in *IEEE Control Systems Magazine*, vol. 19, no. 5, pp. 59-70, Oct. 1999.
- [6] X. Zhao, S. Yin, H. Li and B. Niu, "Switching Stabilization for a Class of Slowly Switched Systems," in *IEEE Transactions on Automatic Control*, vol. 60, no. 1, pp. 221-226, Jan. 2015.
- [7] J. P. Hespanha and A. S. Morse, "Stability of switched systems with average dwell-time," *Proceedings of the 38th IEEE Conference on Decision and Control (Cat. No.99CH36304)*, Phoenix, AZ, USA, 1999, pp. 2655-2660 vol.3.
- [8] S. Liu, A. Tanwani and D. Liberzon, "Average Dwell-Time Bounds for ISS and Integral ISS of Switched Systems using Lyapunov Functions," *2020 59th IEEE Conference on Decision and Control (CDC)*, Jeju, Korea (South), 2020, pp. 6291-6296.
- [9] P. C. Krause, O. Waszczuk, S. D. Sudhoff, *Analysis of Electric Machinery and Drive Systems*, Piscataway, NJ: IEEE press, 2002.
- [10] Z. Zhang, A. M. Bazzi and A. Semin, "An Active Zero-State Switch (AZS) for Commonmode Voltage Reduction in Voltage Source Inverter (VSI) Drives," *2020 IEEE Applied Power Electronics Conference and Exposition (APEC)*, New Orleans, LA, USA, 2020, pp. 711-717, doi: 10.1109/APEC39645.2020.9124003.

[11] Z. Zhang and A. M. Bazzi, "Common-mode Voltage Reduction in VSI-fed Motor Drives with An Integrated Active Zero-state Switch," in *IEEE Journal of Emerging and Selected Topics in Power Electronics*, doi: 10.1109/JESTPE.2020.3037886.

TABLE I. STATE-SPACE REPRESENTATION OF IM DRIVE UNDER V/F CONTROL, IFOC, AND DTC

V/f control	$A_{V/f} = \begin{bmatrix} -R_s / \chi_3 & -\omega_{s0} & -R_s / \chi_1 & 0 & 0 \\ \omega_{s0} & -R_s / \chi_3 & 0 & -R_s / \chi_1 & 0 \\ -R_r / \chi_1 & 0 & -R_r / \chi_2 & \omega_{r0} - \omega_{s0} & \psi_{dr0} \\ 0 & -R_r / \chi_1 & \omega_{s0} - \omega_{r0} & -R_r / \chi_2 & -\psi_{dr0} \\ -H\psi_{dr0} & H\psi_{qr0} & H\psi_{ds0} & -H\psi_{qs0} & 0 \end{bmatrix}$	$B_{V/f} = \begin{bmatrix} -\psi_{ds0} & 0 \\ k + \psi_{qs0} & 0 \\ -\psi_{dr0} & 0 \\ \psi_{dr0} & 0 \\ 0 & -1/J \end{bmatrix}$	$H = 3P / (2J\chi_1)$
	$x_{V/f} = [\psi_{qs} \ \psi_{ds} \ \psi_{qr} \ \psi_{dr} \ \omega_r]^T$	$u_{V/f} = [\omega_s^* \ T_L]^T$	
IFOC	$A_{IFOC} = \begin{bmatrix} 0 & 0 & -1/T_r & -1 & 0 & 0 \\ 0 & 0 & 0 & 0 & -1 & 0 \\ 0 & 0 & 0 & 1 & 0 & 0 \\ k_{i_d} / \chi_3 & 0 & -a_0 / \chi_3 - k_{p_d} / (\chi_3 T_r) & -a_1 / \chi_3 - k_{p_d} / \chi_3 & 0 & 0 \\ 0 & k_{i_q} / \chi_3 & 0 & 0 & -R_s / \chi_3 - k_{p_q} / \chi_3 & 0 \\ 0 & 0 & L_m / T_r^2 & L_m / T_r & 0 & -1/T_r \end{bmatrix}$		
	$B_{IFOC} = \begin{bmatrix} 1/L_m & 0 \\ -WT_{e0} / \psi_{dr0}^2 & W / \psi_{dr0} \\ 0 & 0 \\ k_{p_d} / (\chi_3 L_m) & 0 \\ -Wk_{p_q} T_{e0} / (\chi_3 \psi_{dr0}^2) & Wk_{p_q} / (\chi_3 \psi_{dr0}) \\ 0 & 0 \end{bmatrix}$		$a_0 = R_s / T_r$ $a_1 = R_s + \chi_3 / T_r + L_m / (T_m T_r)$ $W = 4L_r / 3 / P / L_m$
DTC	$x_{IFOC} = [u_{i_d} \ u_{i_q} \ v \ \dot{v} \ i_{qs} \ \psi_{dr}]^T$	$u_{IFOC} = [\psi_{dr}^* \ T_e^*]^T$	
	$A_{DTC} = \begin{bmatrix} 0 & 0 & -1 & 0 \\ 0 & 0 & 0 & 0 \\ k_{i_q} & 0 & -k_{p_q} - R_s / \chi_3 & -R_s / \chi_1 \\ 0 & 0 & -R_r / \chi_1 & -R_r / \chi_2 \end{bmatrix}$	$B_{DTC} = \begin{bmatrix} 1 & 0 \\ 0 & 0 \\ k_{p_q} & 0 \\ 0 & 0 \end{bmatrix}$	
	$x_{DTC} = [u_{\psi} \ u_T \ \psi_{ds} \ \psi_{dr}]^T$	$u_{DTC} = [\psi_{ds}^* \ T_e^*]^T$	